Vol. 74, No. 22

Dependence of Adenovirus Infectivity on Length of the Fiber Shaft Domain

DMITRY M. SHAYAKHMETOV AND ANDRÉ LIEBER*

Division of Medical Genetics, University of Washington, Seattle, Washington 98195

One of the objectives in adenovirus (Ad) vector development is to target gene delivery to specific cell types. Major attention has been given to modification of the Ad fiber knob, which is thought to determine virus tropism. However, among the human Ad serotypes with different tissue tropisms, not only the knob but also the length of the fiber shaft domain varies significantly. In this study we attempted to delineate the role of fiber length in coxsackievirus-adenovirus receptor (CAR)- and non-CAR-mediated infection. A series of Ad serotype 5 (Ad5) capsid-based vectors containing long or short fibers with knob domains derived from Ad5, Ad9, or Ad35 was constructed and tested in adsorption, internalization, and transduction studies. For Ad5 or Ad9 knob-possessing vectors, a long-shafted fiber was critical for efficient adsorption/internalization and transduction of CAR/αv integrin-expressing cells. Ad5 capids containing short CAR-recognizing fibers were affected in cell adsorption and infection. In contrast, for the chimeric vectors possessing Ad35 knobs, which enter cells by a CAR/αv integrin-independent pathway, fiber shaft length had no significant influence on binding or infectibility on tested cells. The weak attachment of short-shafted Ad5 or Ad9 knob-possessing vectors seems to be causally associated with a charge-dependent repulsion between Ad5 capsid and acidic cell surface proteins. The differences between short- and long-shafted vectors in attachment or infection were abrogated by preincubation of cells with polycations. This study demonstrates that the fiber-CAR interaction is not the sole determinant for tropism of Ad vectors containing chimeric fibers. CAR- and αv integrin-mediated infections are influenced by other factors, including the length of the fiber shaft.

Most recombinant adenovirus (Ad) vectors currently used for in vitro and in vivo gene transfer are based on serotype 5 (Ad5). Efficient transduction with these vectors requires the presence of appropriate cell receptors for binding and/or internalization. High-affinity binding of Ad5 is mediated through the coxsackievirus and Ad receptor (CAR) (6, 7, 68). Ad5 internalization requires an additional interaction of RGD motifs on the penton base with $\alpha v\beta 3$ and/or $\alpha v\beta 5$ integrins on the cell surface (32, 39, 48, 71).

Safety and efficacy of in vivo applications of Ad vectors require targeting to specific tissues, which is precluded by the widespread distribution of CAR and αv integrins. On the other hand, a number of tissues, which represent important targets for gene therapy, are refractory to Ad5 infection due to the lack of these receptors (11, 64, 70, 73). Therefore, modification of tropism is one of the central tasks in Ad vector development. One strategy to retarget Ad5 vectors involves complexing the Ad capsid with bispecific antibodies (18, 70) or peptide ligands (17, 58). Another approach is genetic modification of the Ad5 fiber knob (43), which is aimed toward the incorporation of specific peptide ligands into the Ad5 knob with simultaneous abrogation of the natural Ad5 tropism. With the identification of CAR-interacting residues within the Ad5 fiber knob (8, 34, 57) and generation of cell lines for propagation of viruses with abrogated CAR tropism (21, 23, 57), this strategy may soon allow for production of Ad vectors with targeted tropism. A third successful retargeting strategy involves swapping the fiber from one Ad serotype to another serotype with different tissue or receptor tropisms (25, 35, 46, 61, 64, 65, 72, 73). In many of these chimeric vectors, only the fiber knob, which is thought to be the main determinant of viral tropism (29, 42, 65), was exchanged. In human Ads, the rod-like fiber shaft contains repeats of up to 14 amino acids forming β sheets, with the number of repeats ranging from 6 (in Ad3, Ad11, and Ad35) to 23 (in Ad12) (13). The available data do not allow for a clear conclusion to be drawn about the role of fiber shaft length in Ad-host cell interactions. Roelvink et al. suggested that the shorter length of fiber in wild-type Ad9 (8 β sheets; 11 nm) than in wild-type Ad2 fiber (22 β sheets; 37 nm) permitted fiber-independent binding and infection through the direct interaction of penton base with cellular αv integrins (55, 56). However, when the short-shafted Ad9 fiber was incorporated into an Ad5 capsid, the Ad5/9 chimeric vectors showed a dramatic decrease in infectivity of cells expressing CAR and/or αv integrins (26; D. M. Shayakhmetov, unpublished results). Notably, both Ad5 and Ad9 fibers bind to soluble recombinant CAR (55) and require αv integrins for internalization into cells (55, 71). In contrast, another chimeric Ad5/7 vector containing the short-shafted Ad7 fiber, which interacts with a receptor different from CAR, was not affected with regard to infectivity of CAR-replete and CAR-deficient cells (26). Similar results were obtained in our lab with an Ad5/35 chimeric vector containing the short-shafted, non-CAR-binding Ad35 fiber (61). From these data, it appears that at least two factors determine viral infectivity and tropism: (i) the fiber knob-primary receptor interaction and (ii) the length of the fiber shaft. To more systematically analyze the role of fiber length in Ad-host cell interactions, we generated viruses with chimeric fibers containing short or long shafts in combination with CAR (Ad5 and Ad9)- or non-CAR (Ad35)-recognizing knob domains. Virus attachment and internalization as well as viral transduction were tested on cells expressing different levels of CAR and αv integrins.

---

* Corresponding author. Mailing address: Division of Medical Genetics, University of Washington, Seattle, WA 98195. Phone: (206) 221-3973. Fax: (206) 685-8675. E-mail: lieber00@u.washington.edu.
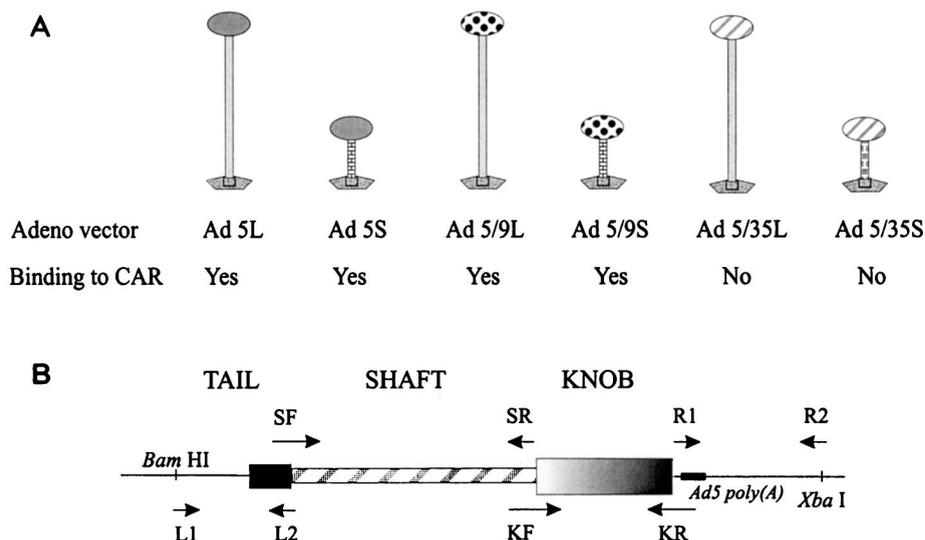
FIG. 1. Schematic representation of chimeric fiber proteins incorporated into Ad5 capsids (A) and structure of chimeric fiber genes (B). (A) The Ad fiber can be divided into three domains. The conserved N-terminal tail contains the sequences responsible for association with the penton base. The long shafts of Ad5L, Ad5/9L, and Ad5/35L contain 22 β sheets (37 nm); the short shafts in Ad5S and Ad5/9S contain 8 β sheets (11 nm); Ad5/35S contains 6 β sheets (9 nm). The C-terminal globular knob domains are derived from Ad5 (Ad5L or -S), Ad9 (Ad5/9L or -S), or Ad35 (Ad5/35L or -S) wild-type viruses. Both Ad5 and Ad9 fibers bind to CAR, whereas Ad35 fiber interacts with an unidentified receptor different from CAR. (B) To construct the corresponding chimeric fiber genes, the indicated sets of primers were used to amplify DNA corresponding to fiber domains derived from different serotypes. To amplify DNA encoding the Ad5 fiber tail domain or the Ad5 fiber gene polyadenylation signal, L1 and L2 primers or R1 and R2 primers, respectively, were used. To amplify DNA encoding the fiber shaft domains, the corresponding shaft forward (SF) and shaft reverse (SR) primers were used. To amplify DNA encoding for the fiber knob domains, the corresponding knob forward (KF) and knob reverse (KR) primers were used. The amplified fiber domains were conjoined with a second PCR step employing primers L1 and R2 as described in Materials and Methods.

MATERIALS AND METHODS

Construction of chimeric Ad vectors. The Ad vectors used in this study possessed long (designated by suffix "L")- or short (designated by suffix "S")-shafted fibers, terminating with knob domains from Ad5, Ad9, or Ad35. Schematic representation of constructed chimeric fiber molecules is shown in Fig. 1A. The detailed structures of Ad5L and Ad5/35S (referred to as Ad5GFP and Ad5GFP/F35, respectively) were described earlier (61). All Ad vectors contain a 2.3-kb, cytomegalovirus promoter-driven enhanced green fluorescent protein (EGFP) gene (derived from pEGFP-1 [Clontech, Palo Alto, Calif.]) inserted into the E3 region of Ad5. The EGFP expression cassette was cloned between Ad5 nt 28191 and 30818 in a shuttle plasmid pE3GFP (61), which contains the E3 deletion described for pBHG10 (Microbix, Toronto, Ontario, Canada). The chimeric fiber gene (Fig. 1B) for each particular Ad vector was constructed by a two-step PCR amplification strategy. During the first step, four DNA fragments corresponding to (i) the 5′ nontranslated region of the fiber gene and fiber tail domain (primers L1 and L2), (ii) the fiber shaft domain (primers SF and SR), (iii) the fiber knob domain (primers KF and KR), and (iv) the Ad5 poly(A) signal followed by about 1,000 bp of Ad5 DNA downstream of the fiber gene (primers R1 and R2) were amplified using Pfu-Turbo DNA polymerase (Stratagene, La Jolla, Calif.). Primer pairs L2 plus SF, SR plus KF, and KR plus R1 were designed to contain complementary sequences of at least 20 nucleotides (nt) in length. During the second step of PCR amplification, these overlapping sequences allowed for joining of the DNA fragments obtained after the first PCR amplification step. To construct complete chimeric fiber genes, the four DNA fragments obtained in the first amplification were agarose gel purified, mixed together, and subjected to a second PCR amplification, using primers L1 and R2. The primer sequences used to construct the chimeric fiber genes were as follows: for Ad5S, SF (nt 31150 to 31177, nt 181 to 208 of Ad9 fiber; 5′-AAT GGG TTT CAA GAG AGT CCC CCT GGA GTC CTG TCA CTC AAA CTA GCT GAC CCA-3′) and SR (nt 32267 to 32245, nt 595 to 571 of Ad9 fiber; 5′-GGA GAT GGA GCT GGT GTG GTC CAT AGG CGG CCC TTA TCT TCT TTT TTA-3′); for Ad5/9L, KF (nt 32220 to 32244, nt 596 to 620 of Ad9 fiber; 5′-CAAA AAT AAT GAT AAG CTA ACT TTG T GGA CAA CTC CAG ACA CAT CTC CAA-3′) and KR (nt 32805 to 32775, nt 1149 to 1113 of Ad9 fiber; 5′-CAT AAC AAC AAC GAT TCT TTA TTC TTG GGC TTC ATT CTT GGG CGA TAT AGG AAA AGG-3′); for Ad5/9S, SF and KR (see above); for Ad5/35L, KF (nt 32215 to 32244, nt 403 to 431 of Ad35 fiber; 5′-GGA AAC AAA AAT AAT GAT AAG CTA ACT TTG TGG ACT GGA ATA AAC CCT CCA CCT AAC TG-3′) and KR (nt 32805 to 32775, nt 991 to 958 of Ad35 fiber; 5′-CAT AAC ACA AAC GAT TCT TTA TTC TTG GGC ATT TTA GTT GTC GTC TTC TGT AAT GTA AG-3′), and for Ad5/35S, SF (nt 31150 to 31177, nt 132 to 159 of Ad35 fiber; 5′-AAT GGG TTT CAA GAG AGT CCC CCT GGA GTT CTT ACT TTA AAA TGT TTA ACC CCA-3′) and KR (nt 32805 to 32775, nt 991 to 958 of Ad35 fiber; 5′-CAT AAC ACA AAC GAT TCT TTA

TTC TTG GGC ATT TTA GTT GTC GTC TTC TGT AAT GTA AG-3′). The underlined numbers refer to the Ad5 genome; the second group of numbers denotes nucleotide positions in the heterologous fiber genes. Ad5 sequences were amplified using the following primers: L1 (contains ClaI and BamHI cloning sites and starts just upstream of Ad5 nt 30818; 5′-CGC GAT ATC GAT TGG ATC CAT TAA CTA-3′), L2 (nt 31174 to 31150; 5′-CAG GGG GAC TCT CTT GAA ACC CAT T-3′), SR for Ad5/9L (nt 32244 to 32220, nt 620 to 596 of Ad9 fiber; 5′-TTG GAG ATG TGT CTG GAG TTG TCC A CAA AGT TAG CTT ATC ATT ATT TTT G-3′), SR for Ad5/35L (nt 431 to 403 of Ad35 fiber, nt 32244 to 32220; 5′-CA GTT AGG TGG AGG GTT TAT TCC AGT CCA CAA AGT TAG CTT ATC ATT ATT TTT GTT TCC-3′), KF (nt 32245 to 32267; 5′-TGG ACC ACA CCA GCT CCA TCT CCT CCT-3′), R1 (nt 32775 to 32805; 5′-GCC CAA GAA TAA AGA ATC GTT TGT GTT ATG-3′), and R2 (nt 33651 to 33621; 5′-AGC TGG TCT AGA ATG GTG GTG GAT GGC GCC A-3′). Nucleotide numbers are given according to the sequences obtained from GenBank (accession no. M73260 and M29978 for Ad5, X74659 for Ad9, and U10272 for Ad35). After the second PCR amplification, the DNA encoding chimeric fiber genes was digested with XbaI and BamHI and inserted into pE3GFP. Finally, chimeric fiber genes were introduced into the Ad5 vector genome using the Escherichia coli recombination system described earlier (9). Correct recombinants were amplified in E. coli HB101 and purified by double CsCl gradient banding. To produce the corresponding viruses, purified plasmids were digested with PacI to release the viral genomes and transfected into 293 cells as described elsewhere (38). Plaques developed 7 to 10 days posttransfection in overlaid cultures. Recombinant viruses were propagated in 293 cells and purified by standard methods described elsewhere (38).

As a source of the heterologous fiber sequences, DNAs extracted from purified wild-type Ad5 (ATCC VR-5), Ad9 (ATCC VR1086), and Ad35 (ATCC VR-716) were used. For amplification, 293 cells were infected with wild-type Ad serotypes under conditions that prevented cross-contamination. Viruses were banded in CsCl gradients, dialyzed, and stored in aliquots as described elsewhere (38).

Ad plaque titers were determined as follows. Confluent 293 cells plated in six-well plates were incubated for 24 h with different dilutions of virus in a total volume of 1 ml. Two weeks after infection, plaques were counted on cultures overlaid with 0.5% agarose–minimal essential medium–10% fetal calf serum (FCS). Ad genome titers were determined by quantitative Southern blotting. To do this, viral DNA extracted from the purified particles was applied to an agarose gel in twofold serial dilutions, together with standard DNA of known concentration (purified Ad5 DNA, whose concentration was determined by measuring optical density at 260 nm). After transfer of DNA onto Hybond N+ nylon membranes (Amersham, Piscataway, N.J.), filters were hybridized with a labeled DNA probe (8-kb HindIII fragment of Ad genome) and DNA concentrations were estimated by PhosphorImager for each particular viral preparation. These

values were then used to calculate the genome titer for each virus stock. For each Ad vector used in this study, at least three independently prepared virus stocks were obtained, PFU and genome titers were determined on 293 cells and by Southern blotting, respectively.

Cell lines. Human embryonic kidney (293) cells (Microbix) were maintained in Dulbecco modified Eagle medium (DMEM)–10% FCS–2 mM glutamine–penicillin-streptomycin. K562 (human erythroleukemia; ATCC 45506) and Y79 (human retinoblastoma; ATCC HTB-18) cells were maintained in RPMI 1640–10% FCS–2 mM glutamine–penicillin-streptomycin (Gibco, BRL). Medium for Y79 cells was additionally supplemented with 1 mM sodium pyruvate, 4.5 g of glucose per liter, and 10 mM HEPES.

Labeling of Ad vectors with [*methyl*-³H]thymidine. Ad vectors were labeled with [*methyl*-^{3}H]thymidine as described in detail elsewhere (56). Briefly, 5×10^7 293 cells were grown in 175-cm² flasks with 15 ml of DMEM–10% FCS and infected with Ad at a multiplicity of infection (MOI) of 50 or higher. Twelve hours postinfection, 1 mCi of [*methyl*-^{3}H]thymidine (Amersham, Arlington Heights, Ill.) was added to the medium, and cells were further incubated at 37°C until complete cytopathic effect was observed. Cells were then harvested, pelleted, washed once with cold phosphate-buffered saline (PBS), and resuspended in 5 ml of PBS. Virus was released from the cells by four freeze-thaw cycles. Cell debris was removed by centrifugation, and viral material was subjected to ultracentrifugation in CsCl gradients and subsequent dialysis as previously described (38). Virion-specific radioactivity as measured by a liquid scintillation counter was in the range of 10^{-5} to 10^{-4} cpm per virion.

Attachment and internalization assays. The assays were performed according to a protocol published earlier (71). For attachment studies, 3.5×10^5 cells were incubated for 1 h on ice with ³H-labeled Ad at an MOI of 8,000 genomes per cell in 100 µl of ice-cold adhesion buffer (DMEM supplemented with 2 mM MgCl$_2$, 1% bovine serum albumin, and 20 mM HEPES). The cells were then pelleted by centrifugation for 4 min at $1,000 \times g$ and washed twice with 0.5 ml of ice-cold PBS. After the last wash, the cells were pelleted at $1,500 \times g$, the supernatant was removed, and the cell-associated radioactivity was determined by a scintillation counter. The number of viral particles bound per cell was calculated using the virion-specific radioactivity and the number of cells. To determine the fraction of internalized ³H-labeled Ad particles, cells were incubated on ice for 1 h with the corresponding virus, washed with PBS as described above, resuspended in 100 µl of adhesion buffer, and then incubated at 37°C for 30 min. Following this incubation, cells were diluted threefold with cold 0.05% trypsin–0.5 mM EDTA solution and incubated at 37°C for an additional 5 to 10 min. This treatment removed 99% of attached radioactivity. Finally, the cells were pelleted at $1,500 \times g$ for 5 min, the supernatant was removed, and the protease-resistant radioactivity was measured. This protocol minimizes the possibility that the internalization data were affected by receptor recycling (54). Nonspecific binding of Ad particles to cells on ice was determined in the presence of 100-fold excess of unlabeled virus. This value routinely represented less than 0.1% of the viral load.

For analysis of virus attachment and/or internalization in the presence of competitors, an infectivity assay was used. The cells were first preincubated with anti-CAR (RmcB [6, 31]; 1/200 dilution) or anti-αv integrin (L230; 1/3 dilution of conditioned medium collected from ATCC HB-8448 hybridoma cell line) monoclonal antibodies at 37°C for 1 h in adhesion buffer. Then antibody-containing medium was removed, indicated amounts of virus were added to cells, and the mixture was incubated at 37°C for another hour. Virus-containing medium was then removed, and the cells were washed once with PBS and incubated for 24 h at 37°C in growth medium.

Ad infection. One day before infection, 2.5×10^5 293 cells were seeded per well (12-well plate). The next day, we determined the number of attached cells per well and added virus at the MOI indicated in the figure legends in 400 µl of growth medium. Cells were incubated for 1 h at 37°C. Next, the virus-containing medium was removed, and the cells were washed once with PBS and incubated in normal medium for 24 h. K562 or Y79 cells growing in suspension were washed twice with PBS before infection and resuspended in growth medium at a concentration of 3×10^6 cells/ml. One hundred microliters of cell suspension was mixed with 50 µl of virus-containing medium. Virus was allowed to attach to cells for 1 h at 37°C. Then the virus-containing medium was removed, and cells were washed once with PBS and incubated for 24 h in normal medium before analysis.

Flow cytometry. Adherent 293 cells grown in non-tissue culture-treated 10-cm-diameter dishes (Falcon, Franklin Lakes, N.J.) were detached by treatment with 1 mM EDTA and washed three times with wash buffer (WB), consisting of PBS supplemented with 1% FCS. Cells grown in suspension (K562 and Y79) were washed three times with WB. After washing, the cells were resuspended in WB at 2×10^6 cells/ml; 2×10^5 cells were incubated in 100 µl of WB for 1 h at 37°C with monoclonal antibodies specific for αv integrins (L230; 1/3 dilution of conditioned medium collected from ATCC HB-8448 hybridoma cell line) or CAR (RmcB; 1/400 final dilution) or with bromodeoxyuridine BrdU (1/100 final dilution; Amersham) as a negative control. Subsequently, cells were washed with WB and incubated with fluorescein isothiocyanate (FITC)-labeled horse anti-mouse immunoglobulin G antibodies (1/100 final dilution; Vector Laboratories, Burlingame, Calif.) for 30 min at 4°C. After incubation with secondary antibodies, cells were washed twice with WB, and 10^4 cells per sample were analyzed in duplicate by flow cytometry.

Hemagglutination (HA) assay. Twenty-five-microliter serial dilutions of Ad stocks in McIlvaine-NaCl buffer (0.1 M citric acid–0.2 M Na$_2$HPO$_4$ [pH 7.2],

TABLE 1. Genome-to-PFU ratios for chimeric Ad vectors[a]

Virus	Genomes/ml (10^{12})	PFU/ml	Genome/PFU ratio
Ad5L	2.2	1.39×10^{11}	13 ± 4.2
Ad5S	1.46	1.04×10^{10}	140 ± 54
Ad5/9L	1.73	6.05×10^{10}	29 ± 6
Ad5/9S	1.28	2.2×10^9	582 ± 158
Ad5/35L	1.6	1.16×10^{11}	14 ± 4.8
Ad5/35S	1.98	1.18×10^{11}	17 ± 6

[a] The genome titers of preparations of purified Ad vectors were measured by quantitative Southern blot analysis (61). The plaque titers were determined on 293 cells under the conditions described in Materials and Methods.

diluted 1:50 with 0.87% NaCl) were loaded onto 96-well plates. To each dilution, 25 µl of a 1% suspension of monkey (for Ad35 knob-possessing vectors) or human (for Ad9 knob-possessing vectors) erythrocytes (in McIlvaine-NaCl buffer) was added. The sedimentation pattern was determined after incubation for 1 h at 37°C. All tests were performed in quadruplicate in at least two independent experiments.

RESULTS

Construction of chimeric Ad vectors. To delineate the role of the fiber length in CAR- and non-CAR-mediated viral infection, we constructed a number of recombinant Ad vectors with Ad5 capsids containing chimeric fibers. These vectors were based on E1/E3-deleted Ad5 genomes, where the endogenous fiber gene was replaced with engineered chimeric fiber genes. The Ad5 backbone was chosen because most recombinant Ad vectors currently used for in vitro and in vivo gene transfer are based on this serotype (28). The chimeric fibers contain the conserved Ad5 tail, short or long shafts, and Ad5, Ad9, or Ad35 knob domains. Both Ad5 and Ad9 knobs bind to CAR (55), whereas the Ad35 knob interacts with an unidentified receptor different from CAR (61). It cannot be excluded that the Ad9 knob interacts also with non-CAR-binding sites, as the natural tropism of Ad9 is different from that of Ad5 (14, 52, 53). For transduction studies, a cytomegalovirus promoter-EGFP gene expression cassette was inserted into the E3 region.

The nomenclature of constructed viruses is as follows. Ad5L and -S contain the Ad5 knob, Ad5/9L and -S contain the Ad9 knob, and Ad5/35L and -S contain the Ad35 knob with long and short shafts, respectively. The long shafts contain 22 β sheets (natural Ad5 fiber shaft). The short shafts for Ad5S and Ad5/9S contain eight (natural Ad9 fiber shaft) or six (natural Ad35 fiber shaft) β sheets for Ad5/35S. Thus, a total of six different vectors were generated (Fig. 1A). Chimeric fiber genes were produced by a two-step PCR method (61) using the primers shown in Fig. 1B. Recombination in *E. coli* was used to replace the Ad5 fiber in pAd.HM4 (47). The recombinant Ad genomes contain the endogenous Ad5 fiber poly(A) signal to terminate transcription of the chimeric fiber genes. The correctness of all Ad genome modifications was confirmed by restriction analysis and sequencing with the primers shown in Fig. 1B. The corresponding chimeric viruses were generated and amplified in 293 cells. The titers of CsCl-banded virus ranged from 1.2×10^{12} to 2.2×10^{12} genomes per ml (Table 1).

A functional test for the presence of heterologous fiber knobs was performed based on HA of human (for Ad9 knob-possessing vectors) or monkey (for Ad35 knob-possessing vectors) erythrocytes. The agglutination of erythrocytes is fiber knob mediated; it is known that Ad5 does not agglutinate erythrocytes whereas Ad9 and Ad35 do so efficiently (3, 41, 52). In HA tests, Ad5/9S or -L and Ad5/35S or -L vectors
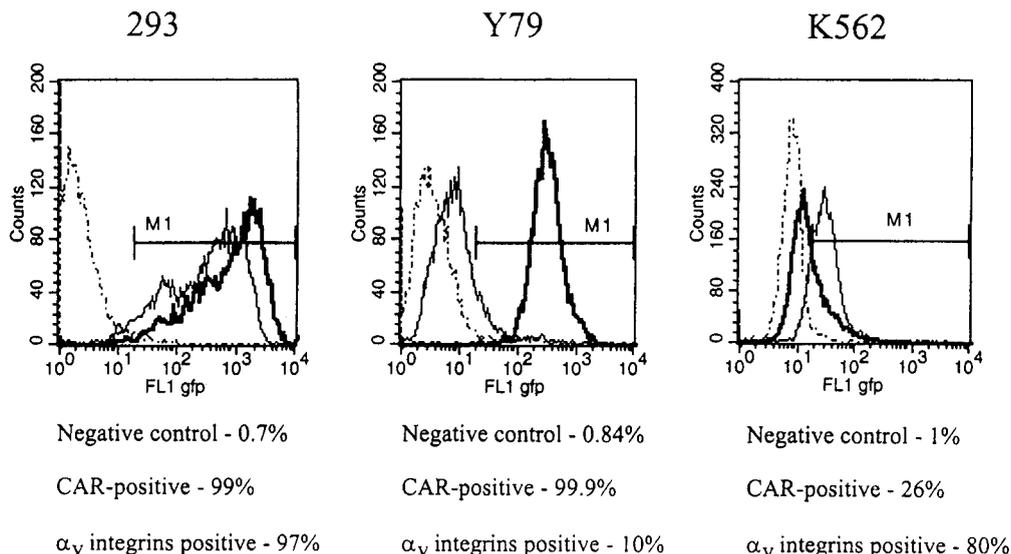
293   Y79   K562

Negative control - 0.7%   Negative control - 0.84%   Negative control - 1%

CAR-positive - 99%   CAR-positive - 99.9%   CAR-positive - 26%

α_V integrins positive - 97% α_V integrins positive - 10% α_V integrins positive - 80%

FIG. 2. Expression of CAR and α_v integrins on 293, K562, and Y79 cells. The level of CAR or α_v integrin expression on test cells was determined by flow cytometry analysis. 293, Y79, and K562 cells were incubated with anti-CAR (RmcB), anti-α_v integrin (L230), or anti-BrdU (as a negative control) primary antibodies as described in Materials and Methods. The binding of primary antibody was developed with anti-mouse IgG-FITC secondary antibody and subsequent flow cytometry analysis for positive staining. The thick, thin, and dotted lines show positive staining with anti-CAR, anti-α_v integrin, and anti-BrdU antibodies, respectively. Data shown represent average results of quadruplicate analyses performed on 10^4 cells. Note that preincubation with the control antibody or with antibody dilution buffer only gave the same intensity of staining (data not shown).

efficiently agglutinated human or monkey erythrocytes, respectively. In contrast, no HA was observed with equivalent Ad5S or -L dilutions (data not shown).

Role of fiber shaft length on levels of attachment and internalization. The attachment of Ad particles to the cell is the first limiting step in virus infection. It has been postulated that for human Ad5, attachment is mediated by high-affinity interactions of the fiber knob domain with its primary cellular receptor, CAR. Efficient internalization of attached particles is mediated by penton base interacting with secondary receptors characterized as cellular α_v integrins. However, it was demonstrated that human Ad9, possessing fibers shorter than Ad5 fibers, can directly interact with cellular integrins, and the role of fiber knob-mediated interactions was considered to be negligible (56).

To study the impact of fiber shaft length on interactions with primary and secondary receptors, we tested attachment and internalization of chimeric viruses on the cell lines that expressed CAR, α_v integrins, or both at high levels. The percentage of CAR- and/or α_v integrins-expressing cells was determined by flow cytometry with specific antibodies (Fig. 2). Almost all of the 293 cells expressed CAR and α_v integrins. Most of the Y79 cells expressed CAR but not α_v integrins. In contrast, the majority of K562 cells were positive for α_v integrins but not for CAR. This selection of test cells also permits investigation of whether short-shafted vectors based on Ad5 capsid can overcome the necessity of binding to CAR by direct interaction with α_v integrins. To analyze attachment of chimeric Ad particles to target cells and subsequent internalization, the vectors were metabolically labeled with [^{3}H]thymidine, which is incorporated into viral DNA during replication. Adsorption and internalization can be experimentally dissociated by taking advantage of the observation that at low temperatures (0 to 4°C) only viral attachment occurs, whereas internalization into cells requires incubation at higher temperatures. The number of particles adsorbed or internalized per

cell was calculated using the virion-specific radioactivity (Fig. 3A). Short- and long-shafted vectors containing the Ad35 knob demonstrated similar strong binding to all cell lines tested. About twice as many particles of the long-shafted, CAR-recognizing Ad5L and Ad5/9L bound to 293 and Y79 cells compared to their short-shafted counterparts. The CAR-binding variants (Ad5 and Ad5/9)—independently of the shaft length—did not interact with the (low-level CAR) K562 cells, suggesting that the short shafts in these capsid chimeras did not confer efficient direct α_v integrin binding and α_v integrin-mediated uptake as described for wild-type Ad9. All bound chimeric particles efficiently internalized into 293 and K562 cells. In Y79 cells, internalization of CAR-interacting vectors was significantly lower, probably due to the low α_v integrin expression. In contrast, for Ad5/35S and Ad5/35L about 95% of attached viral particles were internalized. This is consistent with our previous finding that Ad5/35 chimeric vectors enter cells by a CAR- and α_v integrin-independent pathway (61). The quantitative differences in the number of particles bound to 293 cells was confirmed by direct detection of cell-associated Ad DNA using Southern blotting (Fig. 3B).

The low-level attachment of Ad5/9L compared to Ad5L was rather unexpected, since it has been shown that recombinant soluble fiber knob domains of Ad9 and Ad5 compete with each other for binding to cells with equal efficiency (56). To estimate the effects of the different knob domains on the level of chimeric Ad attachment, we quantitated Ad5L, Ad5/9L, and Ad5/35L binding to 293 cells. All of these vectors had identical Ad5 capsids and natural, long Ad5 fibers but contained different knob domains. Binding studies were performed at different virus concentrations on ice, which precludes positive cooperative binding due to multivalency (12 fibers with three receptor-binding sites per knob [62]), and lateral receptor migration resulting in local aggregates (50). Using Scatchard plots, the apparent association rate constant (K_a) and the number of receptor sites per cell were calculated as described earlier (19,
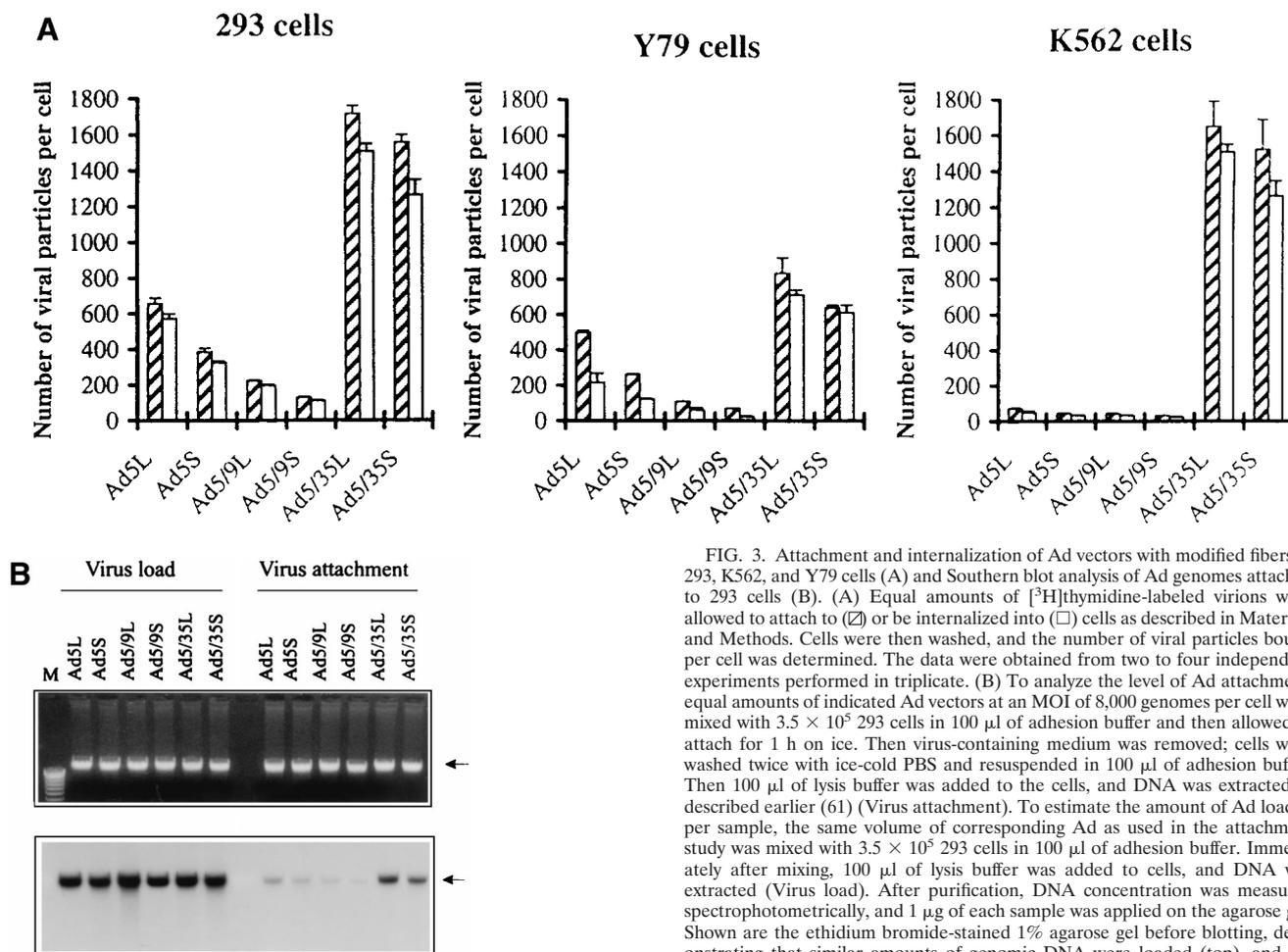
A

B

FIG. 3. Attachment and internalization of Ad vectors with modified fibers to 293, K562, and Y79 cells (A) and Southern blot analysis of Ad genomes attached to 293 cells (B). (A) Equal amounts of [³H]thymidine-labeled virions were allowed to attach to (▨) or be internalized into (□) cells as described in Materials and Methods. Cells were then washed, and the number of viral particles bound per cell was determined. The data were obtained from two to four independent experiments performed in triplicate. (B) To analyze the level of Ad attachment, equal amounts of indicated Ad vectors at an MOI of 8,000 genomes per cell were mixed with 3.5×10^5 293 cells in 100 μl of adhesion buffer and then allowed to attach for 1 h on ice. Then virus-containing medium was removed; cells were washed twice with ice-cold PBS and resuspended in 100 μl of adhesion buffer. Then 100 μl of lysis buffer was added to the cells, and DNA was extracted as described earlier (61) (Virus attachment). To estimate the amount of Ad loaded per sample, the same volume of corresponding Ad as used in the attachment study was mixed with 3.5×10^5 293 cells in 100 μl of adhesion buffer. Immediately after mixing, 100 μl of lysis buffer was added to cells, and DNA was extracted (Virus load). After purification, DNA concentration was measured spectrophotometrically, and 1 μg of each sample was applied on the agarose gel. Shown are the ethidium bromide-stained 1% agarose gel before blotting, demonstrating that similar amounts of genomic DNA were loaded (top), and the result of Southern blot hybridization of the transferred DNA with a ³²P-labeled 8-kb HindIII fragment of the Ad5 genome, corresponding to the E2 region (bottom). The conditions of DNA transfer and hybridization were described earlier (61). M, molecular weight marker. Arrows indicate the Ad DNA (bottom) or mixture of Ad and cellular DNA (top).

20, 50) (Fig. 4). Vectors containing the Ad5- or Ad35-derived knobs bind to their receptors with high affinity, with a K_a comparable to that obtained for Ad2 on HeLa cells (1.0×10^{10} to 2.2×10^{10} M^{-1} [49, 50]). On 293 cells, there were about twice as many high-affinity receptors for Ad35 as for Ad5, which is in agreement with the higher number of bound Ad5/35 particles observed (Fig. 3). The number of Ad5 receptor sites per 293 cells was about 2,600, which is close to the range previously determined for Ad2 on HeLa cells (3,000 to 8,000 [51]). The affinity of Ad5/9L to its receptor(s) on 293 cells was more than 20-fold less than that of Ad5L and Ad5/35L. Although the number of Ad5/9L binding sites was ~9- or ~4-fold higher than the number of Ad5 or Ad5/35 receptors, respectively, this did not compensate for the weak binding observed. The significant difference in number of receptor sites for Ad9 knob-possessing virus compared to the Ad5 knob-possessing counterpart also indicates that the Ad9 knob interacts with at least one receptor besides CAR, which is not recognized by the Ad5 knob. We are now investigating this observation with cell lines that can preferentially be transduced with Ad5/9 vectors but not with Ad5 vectors.

In conclusion, the attachment studies performed on the cell lines expressing different levels of CAR or αv integrins showed that long-shafted, CAR-recognizing Ads were able to attach to and subsequently be internalized by cells consistently more efficiently than their short-shafted counterparts. For Ad5/35, the shaft length did not significantly affect binding to its high-affinity non-CAR receptor.

Transduction properties of chimeric Ad vectors. To test whether varying the fiber shaft length would affect the infectivity of the chimeric Ad vectors, we performed plaque assays on 293 cells and transgene expression studies upon viral infection of 293, Y79, and K562 cells. One of the critical factors that determines the level of viral replication and plaque formation is the number of genomes which enter the nucleus. Therefore, the ratio of the number of genomes added to the cells to PFU is often used to express the infectivity of a given virus (44). The genome-to-PFU ratio determined on 293 cells for CAR-binding, long-shafted viruses was 10-fold (for Ad5) or 20-fold (for Ad5/9) lower than for their short-shafted variants (Ad5S and Ad5/9S) (Table 1). The infectivities of the long- and short-shafted, Ad35 knob-possessing variants were comparable and similar to that of the Ad5L vector.

Overall, results from transduction studies based on analysis of the percentage of GFP-expressing cells mirror the data obtained from adsorption/internalization and plaque assays
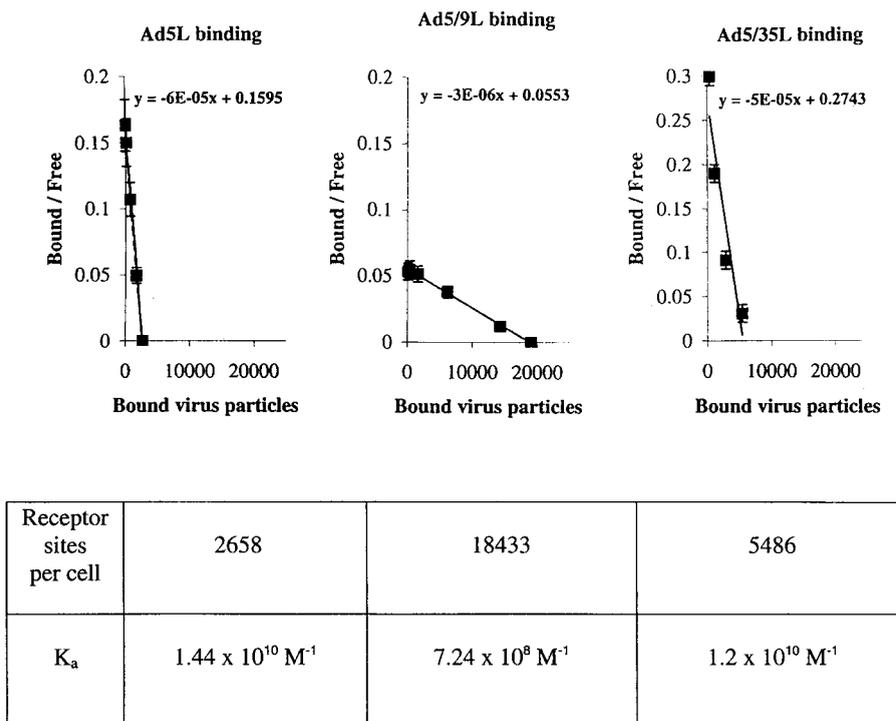
FIG. 4. K_a values of long-shafted Ad variants with different knob domains determined on 293 cells. To analyze the affinity of binding of different knob domains to their receptors, Scatchard plots (59) were made for long-shafted Ad vectors possessing Ad5, Ad9, or Ad35 knob domains. The K_a was calculated based on the slopes of the lines using standard Microsoft Excel software. To ensure binding in equilibrium, different amounts of [³H]thymidine-labeled Ad particles ranging between 2,000 and 200,000 genomes per cell were incubated with 3×10^5 293 cells for 3 h on ice as described in reference 50. For each vector and for each viral concentration, virus attachment was performed in triplicate. The number of receptor sites was extrapolated from the intercept of the lines with the abscissa.

(Fig. 5). In transduction of 293 cells, especially at lower MOIs, the long-shafted, CAR-interacting vectors were clearly superior to Ad5S and Ad5/9S. For example, at an MOI of 20 genomes per cell, the Ad5L vector was able to transduce about 45% of 293 cells, whereas Ad5S transduced only about 7%. Transduction efficiency was comparably high for Ad5/35S and Ad5/35L. Again, the Ad5 and Ad35 knob-possessing viruses infected 293 cells more efficiently than the Ad9 knob-possessing viruses. Interestingly, the long-shafted Ad9 knob-possessing vector (Ad5/9L) showed higher transduction and a lower genome-per-PFU ratio than Ad5S, despite its less efficient attachment to cells (Fig. 3; Table 1). To achieve transduction levels of Y79 or K562 cells comparable to those of 293 cells, at least 100 times more virus was required. In Y79 (low αv integrin) and K562 (low CAR) cells, Ad5/35L and Ad5/35S achieved the highest transduction rates, confirming that Ad5/35 interaction with its receptor allowed for infection by CAR- and αv integrin-independent pathway/s. The low transduction rates of Y79 and K562 cells by CAR-recognizing Ad5 vectors also support earlier observations that high-level expression of only one of the natural Ad receptors (CAR or αv integrins) on the cell surface is not sufficient for efficient cell entry (26). For vectors containing CAR-recognizing fibers (Ad5 and Ad5/9), the long-shafted variants transduced cells more efficiently than their short-shafted counterparts.

The almost negligible infectivity of Ad5S and Ad5/9S on K562 cells corroborates the data obtained in adsorption studies, suggesting that short fibers within the Ad5 capsid cannot overcome the necessity of binding to CAR by direct interaction with αv integrins as suggested earlier (56). To additionally support this statement and demonstrate that CAR and αv integrins are utilized by Ad5 and Ad9 knob-possessing vectors,

we infected 293 cells in the presence of anti-CAR or anti-αv integrin antibodies and then analyzed the percentage of GFP-expressing cells (Fig. 6). Significant reduction in transduction by anti-CAR or anti-αv integrin antibodies was observed for both the long and short Ad5 and Ad5/9 vectors, indicating that CAR and αv integrins are indeed involved in infection with these vectors. Infection with Ad5/35S and Ad5/35L was not significantly affected by CAR antibodies, whereas internalization of Ad5/35L was partially dependent on αv integrins. (Notably, the rate of inhibition of infection by anti-CAR or anti-αv integrin antibodies is in agreement with earlier studies [56, 61].)

Transduction properties of chimeric vectors in the presence of polycations or a cationic lipid. In earlier studies, we demonstrated that wild-type Ad9, containing a short fiber, allowed for efficient attachment and infection of K562 cells, which are rather resistant to wild-type Ad5 infection (61). However, when the same short-shafted Ad9 fiber was transplanted into an Ad5 capsid, cell attachment of this virus chimera decreased dramatically to a lower level than either parental virus (Ad5 or Ad9). We hypothesized that differences in capsid proteins other than fiber may account for this phenomenon. Hexon capsomer is a homotrimer, which covers most of the Ad capsid. Hexon contains three surface loops (L1, L2, and L4) facing outward, of which the hypervariable region 1 (HVR1) in L1 exhibits the greatest variability (5, 16). Protein sequence alignment of hexons from different serotypes revealed that the Ad5 hexon is unusually acidic in its HVR1 loop compared to Ad9 (Fig. 7). Interestingly, for other CAR-recognizing serotypes (Ad9, Ad8, Ad37, and Ad12) including those with short fibers (Ad8, Ad9, and Ad37), either the negatively charged region
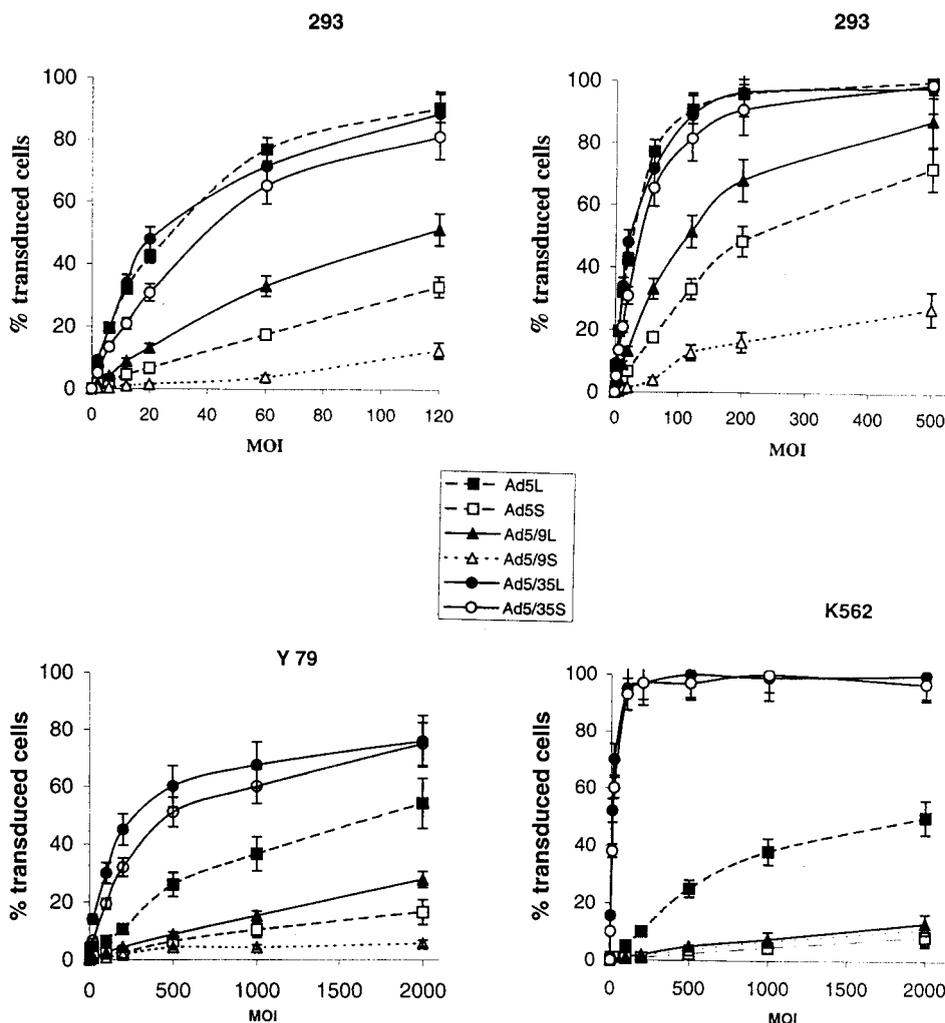
FIG. 5. Transduction of 293, K562, and Y79 cells with chimeric Ad. Cells were infected with different MOIs (viral genomes per cell) for 1 h at 37°C. Virus-containing medium was removed, and cells were incubated in growth medium for 24 h before the percentage of GFP-positive cells was determined by flow cytometry. All infections were done in triplicate in at least two independent settings.

within HVR1 seen in Ad2 and Ad5 is missing (Ad9, Ad12, and Ad37) or the overall charge is positive (Ad8) (16).

Because the exposed regions in the Ad5 hexon were strikingly negatively charged, we speculated that one of the reasons for the weak attachment of Ad5S and Ad5/9S could be an electrostatic repulsion between the Ad5 virion body and acidic cell surface proteins (1). This interference could be more pronounced for the short-shafted, CAR-recognizing Ad5S and Ad5/9S vectors than for the long-shafted variants where the Ad5 hexon-containing capsid is at a greater distance from the cell surface. To support this hypothesis, we attempted to neutralize negative charges on the cell surface by preincubating cells with polycations or cationic lipids.

Preincubation of 293 cells with Polybrene, a ~7,500-Da polycation that has been previously used to neutralize anionic charges on the cell surface (63), completely abrogated the disadvantages of short-shafted Ad5S and Ad5/9S vectors in cell binding, resulting in binding rates comparable to those for Ad5L and Ad5/9L (Fig. 8A). For all vectors tested, the overall number of bound particles was greatly increased, indicating that Polybrene facilitated primary virus attachment. This indicates that in the absence of Polybrene not all of the potential cellular receptors were utilized. Polybrene increased attachment of Ad5/35L and -S or Ad5L only 1.1 to 1.5-fold, whereas it enhanced Ad5/9L and Ad5/9S attachment 4- and 10-fold, respectively. The greater increases in attachment for Ad9 knob-possessing vectors than for Ad5 knob vectors were not unexpected because more Ad9 receptors than Ad5 receptors were present on 293 cells (Fig. 4). Transduction of 293 cells was also increased for CAR-binding Ads in the presence of Polybrene, with the highest increase for Ad5/9S (Fig. 8B). Figure 8C shows GFP expression in 293 cells after transduction with chimeric vectors with or without Polybrene preincubation.

In previous studies, it was shown that polycations improved binding and uptake of standard Ad5-based vectors (15, 33, 36, 40). In these reports, a number of hypotheses were proposed to explain this phenomenon, including polycation-mediated increase in cell permeability, changes in cellular metabolism or receptor expression, or neutralization of serum factors that interfere with Ad binding. It has also been postulated that polycations can provide an "electrostatic bridge" between negatively charged cell membranes and negatively charged domains on Ad capsids. Based on the finding that preincubation with Polybrene predominantly increased the adsorption of
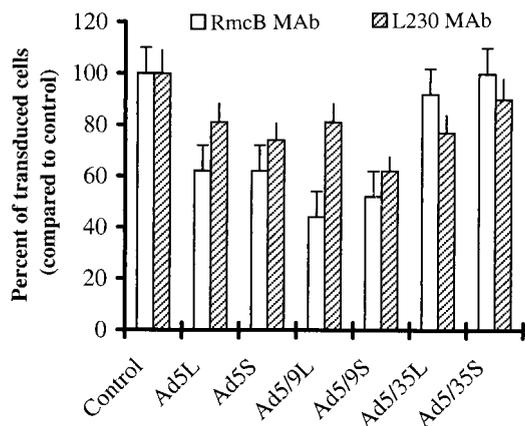
FIG. 6. Effects of anti-CAR and anti-αv antibody on the transduction properties of Ad vectors. 293 cells (3.5×10^5) were preincubated for 1 h at 37°C with anti-CAR (RmcB) or anti-αv integrin (L230) monoclonal antibodies and then incubated with indicated Ad vectors at an MOI of 20 genomes per cell (for Ad5L, Ad5S, Ad5/9L, Ad5/35L, and Ad5/35S) or 100 genomes per cell (Ad5/9S) for 1 h. Virus-containing medium was then removed, and the cells were incubated at 37°C for 24 h in growth medium before the percentage of GFP-positive cells was estimated by flow cytometry. As a control, cells were preincubated with an irrelevant anti-BrdU monoclonal antibody for 1 h before infection. A statistically significant decrease in the percentage of GFP-positive cells was found in infections with chimeric viruses, after preincubation of cells with anti-CAR (for Ad5L, Ad5S, Ad5/9L, and Ad5/9S) or anti-αv integrin (for Ad5L, Ad5S, Ad5/9L, Ad5/9S, and Ad5/35L) monoclonal antibodies ($n = 6$; $P < 0.1$). Notably, preincubation with the control antibody (Control) or with antibody dilution buffer only gave the same percentage of GFP-expressing cells (data not shown).

CAR-interacting chimeric Ad vectors under conditions that did not allow for virus internalization (0°C) (Fig. 8A), we hypothesized that Polybrene specifically enhances binding to CAR. To test this, binding studies were performed in the presence of specific anti-CAR antibodies. The elevated attachment seen for the CAR-recognizing vectors mediated by Polybrene can be blocked by anti-CAR antibodies, demonstrating that binding to CAR remains the primary mechanism of attachment for these vectors to cells in the presence of Polybrene (Fig. 9).

To consolidate these data, we performed similar binding studies in the presence of other polycations, which were different from Polybrene in structure and molecular weight (Fig. 10). Preincubation of cells with protamine sulfate or the cat-

ionic lipid Lipofectamine had effects similar to those seen with Polybrene treatment. Again, competition assays with anti-CAR antibodies demonstrated that increased binding was in large part based on CAR-dependent mechanisms.

In conclusion, short-shafted, CAR-binding vectors do not enter cells as efficiently as their long-shafted counterparts, presumably due to a charge-dependent repulsion between Ad5 hexon and acidic cell surface proteins. Neutralization of negative cell surface charges by preincubation of cells with Polybrene abrogates the differences between short- and long-shafted fiber-containing viruses in attachment or infection. Interaction with CAR remains a predominant mechanism of attachment for these viruses in the presence of polycations or cationic lipids.

DISCUSSION

The goal of this study was to investigate the role of the Ad fiber length in CAR- and non-CAR-mediated infection. To this end, we utilized Ad5 capsid-based vectors containing long or short fibers with knob domains derived from Ad5, Ad9 (CAR binding), and Ad35 (non-CAR binding). Long-shafted, CAR-recognizing vectors attached to and were internalized by cells more efficiently than their short-shafted counterparts. For Ad5/35, shaft length did not significantly affect binding to its high-affinity receptor on the cell lines tested. The chimeric vectors differed also in their infectivity of test cells. Compared to the long-shafted variants, infectivity of short-shafted, CAR-recognizing vectors was at least ~20- or ~4-fold less by plaque assay or GFP expression in 293 cells, respectively. This discrepancy between the assay systems could be due to the fact that viral replication and thus plaque formation start only at a certain threshold concentration of intranuclear viral genomes, whereas transgene expression is usually proportional to the copy number of viral DNA taken up by the cell. Both the long- and short-shafted Ad5/35 vectors efficiently infected cells in a CAR- and αv integrin-independent manner.

Ad5 and Ad5/9 vectors could infect Y79 (low αv integrins) or K562 (low CAR) cells only at very high MOIs, indicating that high-level expression of only one of the natural Ad receptors (CAR or αv integrins) on the cell surface does not allow for efficient infection with CAR-interacting vectors independently of the length of the fiber shaft domains. The necessity of both fiber-CAR and penton-integrin interactions for efficient Ad5 infection is supported by the observation that the infec-
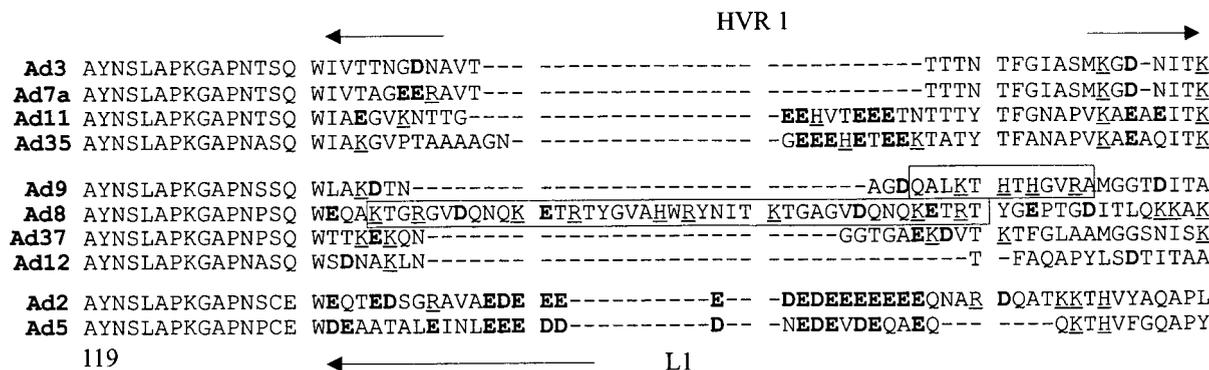

FIG. 7. Amino acid alignments of HVR1 in hexons from different Ad serotypes. Amino acid sequence alignments were done using the ClustalW 1.8 Global progressive algorithm at BCM Search Launcher (http://dot.imgen.bcm.tmc.edu:9331/multi-align). The different human Ad hexon protein sequences were obtained from the NCBI Protein Entrez data bank. Negatively charged amino acids are in bold, and positively charged residues are underlined. Stretches of positively charged amino acids in Ad8 and Ad9 hexon are boxed.
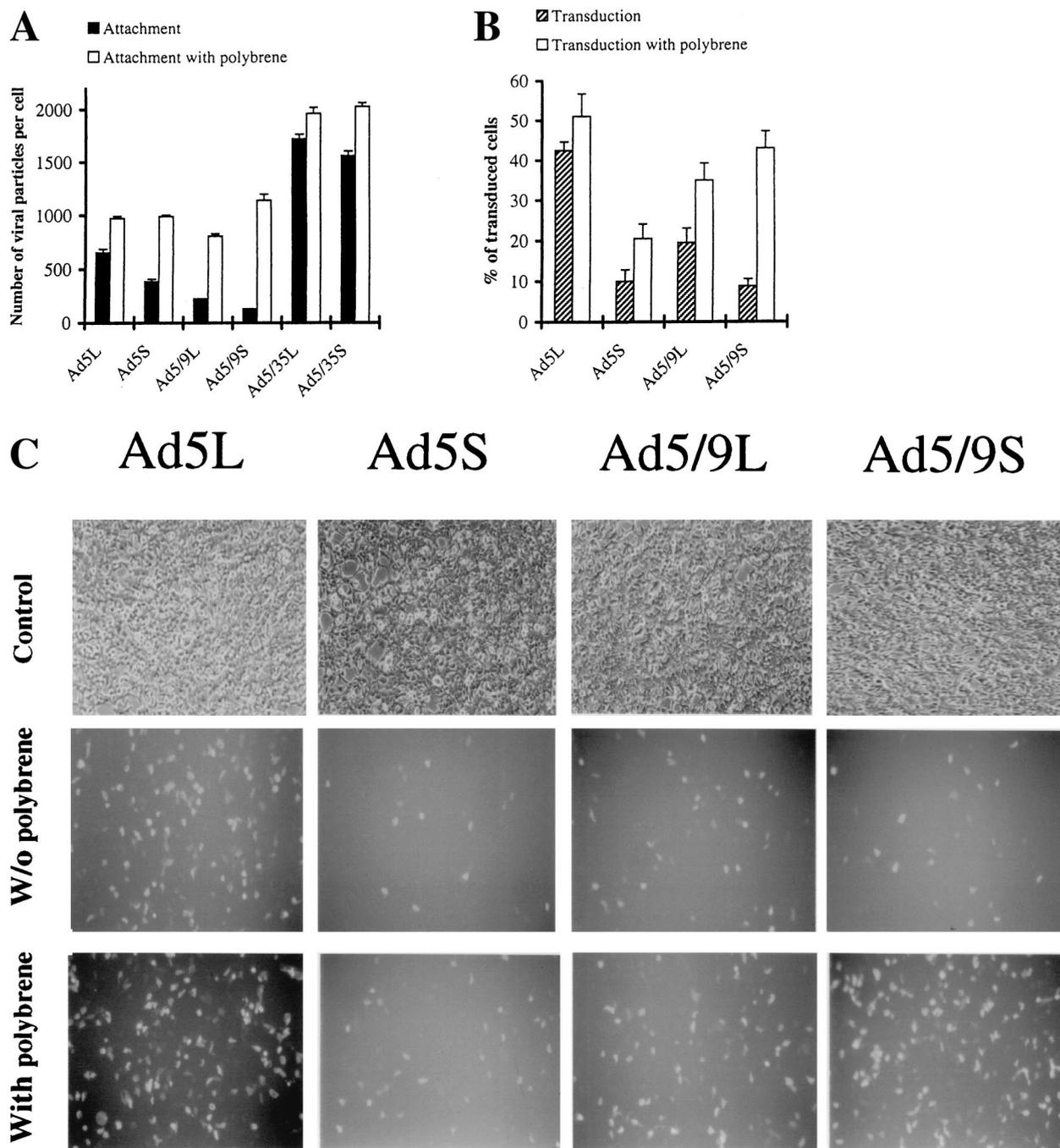
FIG. 8. Attachment of chimeric Ad vectors to 293 cells (A) and transduction of 293 cells with chimeric, CAR-binding Ad vectors (B and C) in the presence of Polybrene. (A) For attachment studies, 3.5×10^5 293 cells were incubated for 1 h on ice in 100 μl of adhesion buffer containing Polybrene (4 μg/ml). Then 25 μl of virus-containing medium was added to the cells (at a final MOI of 8,000 genomes per cell), and virus was allowed to attach for 1 h on ice. Cells were washed twice with PBS, and cell-associated radioactivity was measured $n \geq 3$. (B) For transduction studies, 2.5×10^5 293 cells per well (12-well plate) were incubated with 400 μl of adhesion buffer containing Polybrene (4 μg/ml) at 37°C for 1 h. Then virus-containing medium (total volume of 100 μl) was added to cells. The final MOIs were 20 genomes per cell for Ad5L, Ad5S, and Ad5/9L and 100 genomes per cell for Ad5/9S. Virus was allowed to infect cells for 1 h at 37°C, and then the virus-containing medium was substituted with fresh medium; 24 h postinfection, cells were trypsinized, and the percentage of GFP-positive cells was determined by flow cytometry. (C) 293 cells infected in the presence of Polybrene with Ad vectors possessing modified fiber proteins 24 h postinfection. Cells were infected at MOIs and under the conditions described for panel B. Representative fields with comparable cell densities are shown for each variant. Magnification, ×400.

tivity of fiberless (37, 69) or RGD-deficient (4, 26) vectors was greatly diminished.

Recently, Roelvink et al. demonstrated that the Ad9 fiber knob binds to CAR (55). However, Ad9 infection was not inhibited by competing soluble fiber, whereas antibodies to αv

integrins or penton base did block binding (56). From this observation, they concluded that the shorter length of fiber in wild-type Ad9 than in wild-type Ad5 permitted fiber-independent binding of Ad9 penton base to αv integrins. They also suggested that generation of Ad5 recombinants with short
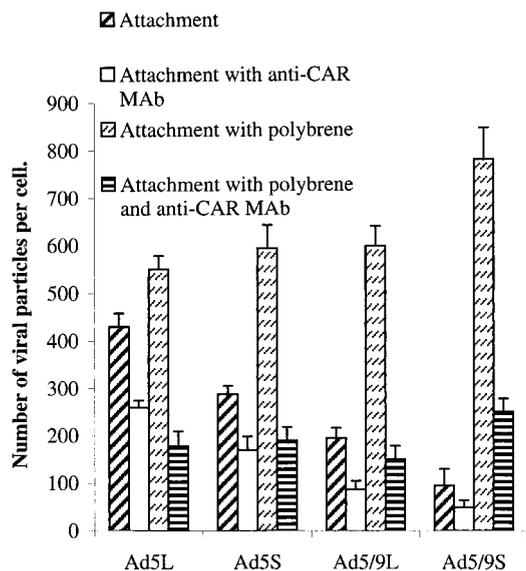
FIG. 9. Attachment of chimeric Ad vectors to 293 cells in the presence of Polybrene and anti-CAR monoclonal antibody. 293 cells (3.5×10^5) were incubated in 100 μl of adhesion buffer without any competitors, with anti-CAR (RmcB monoclonal antibody; 1/200 dilution), with Polybrene (final concentration, 4 μg/ml), or with anti-CAR antibody and Polybrene together for 1 h on ice. Then Ad was added at an MOI of 4,000 genomes per cell in a total volume of 25 μl. Viruses were allowed to attach to cells for 1 h. After washing with ice-cold PBS, cells were pelleted, cell-associated radioactivity was measured, and the number of viral particles attached per cell was calculated for each virus. All attachment studies were performed in triplicate in at least two independent experiments.

shafts would confer targeting Ad vectors directly to αv integrins, allowing for efficient infection by a CAR-independent pathway (55, 56). Our data contradict this suggestion; Ad5 vectors with short-shafted fibers possessing Ad5 or Ad9 knobs demonstrated significantly decreased attachment and infectivity compared to their long-shafted counterparts. This indicates that there was no efficient binding to αv integrins capable of bypassing the high-affinity fiber knob-mediated interaction with CAR. We propose two hypotheses (not mutually exclusive) to explain this discrepancy as well as the observed differences between short- and long-shafted CAR-binding vectors. In our studies, the short-shafted Ad9 fiber was implanted into an Ad5 capsid, which may have properties different from those of the wild-type Ad9 capsid, particularly in the penton and hexon proteins. Based on the fact that both fiber CAR and RGD integrin interactions are required for efficient Ad5 infection (71), our first hypothesis assumes that a correct spatial arrangement of knob and penton RGD motifs is critical for efficient viral binding and entry. The RGD motif is positioned in the center of a protruding loop, which varies in length among serotypes (12). Therefore, the natural spatial arrangement is disturbed when short-shafted heterologous fibers are inserted into the Ad5 capsid. To achieve infectivity comparable to that possible with wild-type Ad5, vectors with Ad5 pentons and chimeric, CAR-interacting fibers require long, natural Ad5 shafts to maintain the appropriate distance between the penton-localized RGD motif and CAR-binding knob. Our studies with long- and short-shafted Ad5 and Ad5/9 vectors support this hypothesis. Our second hypothesis is based on the observation that exposed loops within the Ad5 hexon are highly negatively charged compared to other CAR-interacting, short-shafted Ad serotypes (e.g., Ad8 and Ad9). In Ad5S and Ad5/9S

with short-shafted fibers in Ad5 capsids, a charge-dependent repulsion between Ad5 hexon and acidic cell surface proteins could prevent the high-affinity (CAR or αv integrin)-mediated binding. Correspondingly, this repulsion would be less pronounced in long-shafted vectors. This may allow for more efficient fiber-CAR interactions because the virion body is at a greater distance from the cell surface. This hypothesis was supported by our findings that neutralization of negative cell surface charges by preincubation of cells with polycations abrogated the differences between short- and long-shafted fibers in attachment or infection. There are numerous reports showing that treatment with polycations or enzymatic removal of negatively charged cellular glycoconjugates can significantly improve the level of Ad-mediated gene transfer (1, 15, 17, 22, 30, 33, 36, 40). Our data may provide an explanation for the mechanism behind this phenomenon. The problem of electrostatic interference in Ad binding and infection could be relevant for in vivo application of Ad5-based vectors because acidic residues in cell membranes or extracellular matrix (e.g., sialic acids or sulfated proteoglycans) are common in many tissues. Therefore, electrostatic interference could play an important role in determining the in vivo tropism of Ad5 vectors along with the level of cellular CAR and αv integrin expression. In this context, Fechner et al. reported recently that neither αv integrins nor CAR expression correlates with Ad5-based vector targeting after systemic vector application (24). Proof of our repulsion hypothesis requires additional experiments including the construction of a chimeric hexon virus that does not contain acidic residues in its exposed loops.

The binding studies suggest that Ad5/9L is able to interact with CAR as well as with another receptor on 293 cells because the number of receptor-binding sites for Ad5/9L was 10 times higher than for Ad5L (Fig. 4). Interestingly, despite less efficient attachment of Ad5/9L than of Ad5S (Fig. 3), Ad5/9L infectivity was remarkably higher than that of Ad5S (Fig. 5; Table 1). The lower degree of Ad5/9L attachment to its receptors might be compensated for by a higher efficiency of subsequent steps in infection such as intracellular trafficking or endosome escape. Differences in intracellular trafficking may also explain why transduction with Ad5S in the presence of Polybrene did not proportionally increase with the greater adsorption rates of Ad5S. This hypothesis should be proved by additional studies. In this context, earlier reports have shown that the Ad fiber plays a critical role not only in viral attachment but also in intracellular trafficking (46) and endosome escape (45). The binding constants for Ad5L and for Ad5/9L, both containing the natural Ad5 capsid and fiber shaft but different knobs, differed by more than a factor of 20. This is in conflict with earlier reports showing that soluble Ad5 and Ad9 fibers crosscompete with similar affinities for binding to the cellular receptor (56). In our system, we used complete virions as well as different test cells, which may account for this discrepancy.

For the Ad35 knob-possessing vectors which infected cells by a CAR-independent pathway (61), the length of the fiber shaft appeared to be not critical for infection of the cell lines tested. Another chimeric Ad5/7 vector containing the short-shafted Ad7 fiber, which also interacts with a receptor different from CAR, was not affected in its infectivity of CAR-replete and CAR-deficient cells (26). There are probably two different receptors for Ad7 (subgroup B:1) and Ad35 (subgroup B:2), with tropism for the respiratory and urinary tracts, respectively (29, 60). The cellular receptor for Ad35 remains to be identified. From earlier studies, we know that this receptor is expressed on hematopoietic cells including human CD34$^+$ and K562 cells (60, 61). Binding to this receptor may be sufficient for internalization because αv integrins were not required for
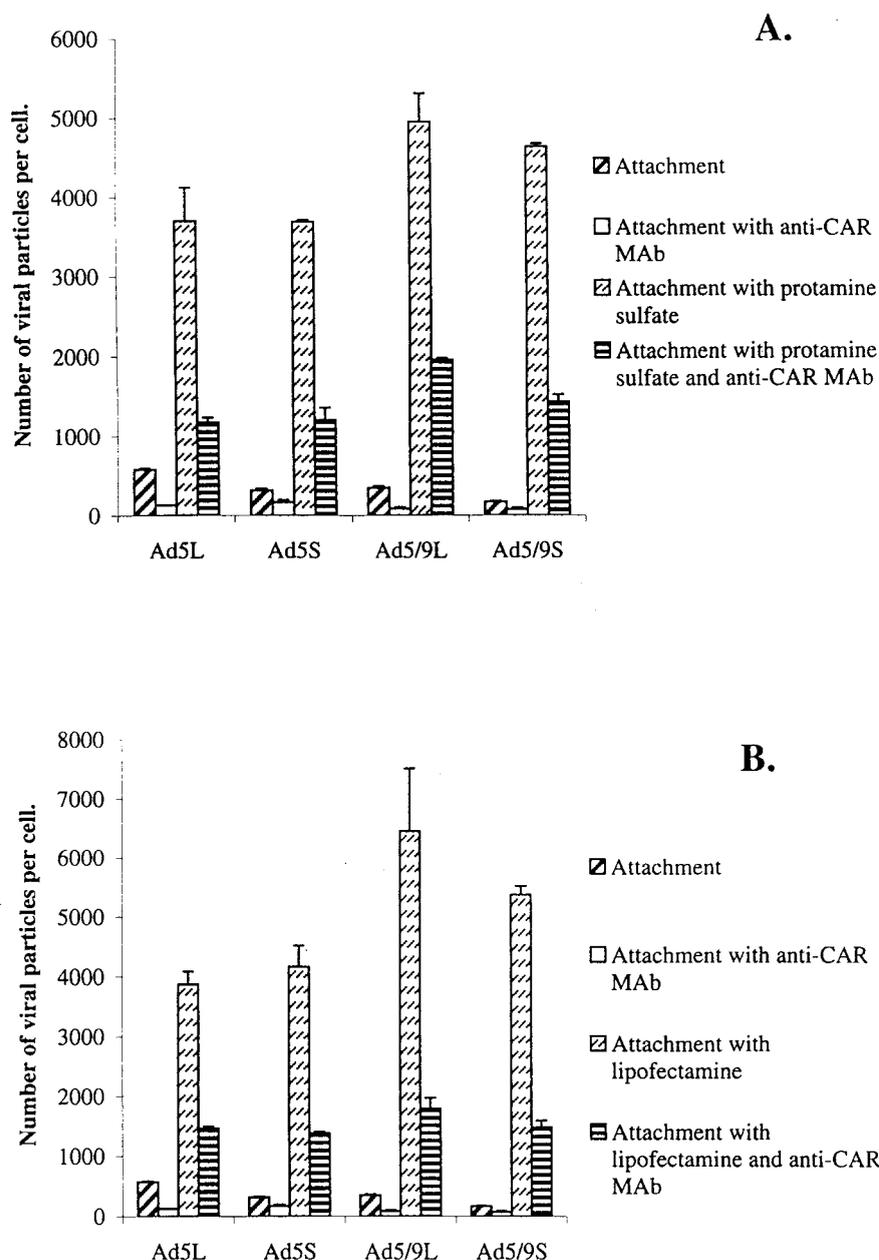
FIG. 10. Attachment of chimeric Ad vectors to 293 cells in the presence of protamine (A) or Lipofectamine (B). Adsorption studies were performed as described for Fig. 9. The concentrations of protamine sulfate and the cationic lipid Lipofectamine were 400 and 50 μg/ml, respectively. All attachment studies were performed in triplicate in at least two independent experiments.

Ad5/35 in infection of human CD34$^+$ cells (61). Ad5/35 binds to its receptor with an affinity comparable to that of Ad5 interaction with CAR (Fig. 4). However, while both long- and short-shafted Ad5/35 vectors infect cells efficiently, the short-shafted CAR-interacting (Ad5 and Ad5/9) vectors do not. Interestingly, the wild-type Ad35 capsid contains short-shafted fibers and hexons with negative charges within HVR1 similar to the Ad5 hexons. This might explain why the Ad5/35S chimera demonstrated efficient binding and internalization properties similar to those of the wild-type Ad35 (61). We speculate that the Ad35 knob, unlike that of Ad5 or Ad9, recognizes a receptor that is elevated above the cellular (acidic) glycocalyx, which reaches only 10 nm above the cell surface (27). This

receptor could represent glycoproteins, membrane components that often tower 200 to 300 nm above the glycocalyx (27). Among the viruses that interact with sialylated glycolipids (gangliosides) or glycoproteins on target cell membranes are influenza virus, parvovirus, and polyomavirus (10, 66, 67). Recently, it was found that Ad37 (subgenus D) uses specific α(2→3) sialic acids on membrane glycoproteins for attachment and entry (2). On the other hand, the efficient binding of Ad5/35S and Ad5/35L to 293 cells could be due to the higher number of Ad35 receptors so that the difference in attachment between short- and long-shafted adenoviruses becomes less significant. Alternatively, since Ad5/35 binds to a receptor allowing for internalization without the need for integrins, fiber

length may not be as critical as for Ad5 and Ad5/9, which require interaction with two cellular receptors for efficient uptake. In this context, it is notable that the effectiveness of a high-affinity ligand inserted into penton base was similar to that of one inserted into fiber when an internalizing receptor was targeted (23).

The utility of Ad vectors for gene therapy can be improved by the development of viruses with specifically altered tropisms. Particularly, vectors with high affinity for specific target cells can be used at lower concentrations, which would reduce in vivo cytotoxicity related to systemic Ad vector application. Our study contributes to a better understanding of factors responsible for successful Ad-target cell interactions, which govern both natural and modified Ad tropisms. It demonstrates that for the widely used Ad5 capsid-based vector, fiber length is an important factor that should be considered in the construction of tropism-modified vectors for in vitro and in vivo gene transfer.

ACKNOWLEDGMENTS

REFERENCES

1. **Arcasoy, S. M., J. Latoche, M. Gondor, S. C. Watkins, R. A. Henderson, R. Hughey, O. J. Finn, and J. M. Pilewski.** 1997. MUC1 and other sialoglyco-conjugates inhibit adenovirus-mediated gene transfer to epithelial cells. Am. J. Respir. Cell Mol. Biol. **17:**422–435.
2. **Arnberg, N., K. Edlund, A. H. Kidd, and G. Wadell.** 2000. Adenovirus type 37 uses sialic acid as a cellular receptor. J. Virol. **74:**42–48.
3. **Arnberg, N., Y. Mei, and G. Wadell.** 1997. Fiber genes of adenoviruses with tropism for the eye and the genital tract. Virology **227:**239–244.
4. **Bai, M., B. Harfe, and P. Freimuth.** 1993. Mutations that alter an Arg-Gly-Asp (RGD) sequence in the adenovirus type 2 penton base protein abolish its cell-rounding activity and delay virus reproduction in flat cells. J. Virol. **67:**5198–5205.
5. **Bailey, A., and V. Mautner.** 1994. Phylogenetic relationships among adenovirus serotypes. Virology **205:**438–452.
6. **Bergelson, J. M., J. A. Cunningham, G. Droguett, E. A. Kurt-Jones, A. Krithivas, J. S. Hong, M. S. Horwitz, R. L. Crowell, and R. W. Finber.** 1997. Isolation of a common receptor for coxsackie B viruses and adenoviruses 2 and 5. Science **275:**1320–1323.
7. **Bergelson, J. M., A. Krithivas, L. Celi, G. Droguett, M. S. Horwitz, T. Wickham, R. L. Crowell, and R. W. Finberg.** 1998. The murine CAR homolog is a receptor for coxsackie B viruses and adenoviruses. J. Virol. **72:**415–419.
8. **Bewley, M. C., K. Springer, Y. B. Zhang, P. Freimuth, and J. M. Flanagan.** 1999. Structural analysis of the mechanism of adenovirus binding to its human cellular receptor, CAR. Science **286:**1579–1583.
9. **Chartier, C., E. Degryse, M. Gantzer, A. Dieterle, A. Pavirani, and M. Mehtali.** 1996. Efficient generation of recombinant adenovirus vectors by homologous recombination in *Escherichia coli*. J. Virol. **70:**4805–4810.
10. **Chen, M. H., and T. Benjamin.** 1997. Roles of N-glycans with alpha2,6 as well as alpha2,3 linked sialic acid in infection by polyoma virus. Virology **233:**440–442.
11. **Chillon, M., A. Bosch, J. Zabner, L. Law, D. Armentano, M. Welsh, and B. L. Davidson.** 1999. Group D adenoviruses infect primary central nervous system cells more efficiently than those from group C. J. Virol. **73:**2537–2540.
12. **Chiu, C. Y., P. Mathias, G. R. Nemerow, and P. L. Stewart.** 1999. Structure of adenovirus complexed with its internalization receptor, $\alpha v \beta 5$ integrin. J. Virol. **73:**6759–6768.
13. **Chroboczek, J., R. W. H. Ruigrok, and S. Cusack.** 1995. Adenovirus fiber, p. 163–200. *In* P. B. W. Doerfler (ed.), The molecular repertoire of adenoviruses, vol. 1. Springer-Verlag, Berlin, Germany.
14. **Chroboczek, J., and B. Jacrot.** 1987. The sequence of adenovirus fiber: similarities and differences between serotypes 2 and 5. Virology **161:**549–554.
15. **Clark, P. R., A. T. Stopeck, J. L. Brailey, Q. Wang, J. McArthur, M. H. Finer, and E. M. Hersh.** 1999. Polycations and cationic lipids enhance adenovirus transduction and transgene expression in tumor cells. Cancer Gene Ther. **6:**437–446.
16. **Crawford-Miksza, L., and D. P. Schnurr.** 1996. Analysis of 15 adenovirus

hexon proteins reveals the location and structure of seven hypervariable regions containing serotype-specific residues. J. Virol. **70:**1836–1844.
17. **Curiel, D. T.** 1994. High-efficiency gene transfer employing adenovirus-poly-lysine-DNA complexes. Nat. Immun. **13:**141–164.
18. **Curiel, D. T., S. Agarwal, E. Wagner, and M. Cotten.** 1991. Adenovirus enhancement of transferrin-polylysine-mediated gene delivery. Proc. Natl. Acad. Sci. USA **88:**8850–8854.
19. **Davison, E., I. Kirby, T. Elliott, and G. Santis.** 1999. The human HLA-A*0201 allele, expressed in hamster cells, is not a high-affinity receptor for adenovirus type 5 fiber. J. Virol. **73:**4513–4517.
20. **Defer, C., M. T. Belin, M. L. Caillet-Boudin, and P. Boulanger.** 1990. Human adenovirus-host cell interactions: comparative study with members of subgroups B and C. J. Virol. **64:**3661–3673.
21. **Douglas, J. T., C. R. Miller, M. Kim, I. Dmitriev, G. Mikheeva, V. Krasnykh, and D. T. Curiel.** 1999. A system for the propagation of adenoviral vectors with genetically modified receptor specificities. Nat. Biotechnol. **17:**470–475.
22. **Dunphy, E. J., R. A. Redman, H. Herweijer, and T. P. Cripe.** 1999. Reciprocal enhancement of gene transfer by combinatorial adenovirus transduction and plasmid DNA transfection in vitro and in vivo. Hum. Gene Ther. **10:**2407–2417.
23. **Einfeld, D. A., D. E. Brough, P. W. Roelvink, I. Kovesdi, and T. J. Wickham.** 1999. Construction of a pseudoreceptor that mediates transduction by adenoviruses expressing a ligand in fiber or penton base. J. Virol. **73:**9130–9136.
24. **Fechner, H., A. Haack, H. Wang, X. Wang, K. Eizema, M. Pauschinger, R. Schoemaker, R. Veghel, A. Houtsmuller, H. P. Schultheiss, J. Lamers, and W. Poller.** 1999. Expression of coxsackie adenovirus receptor and αv-integrin does not correlate with adenovector targeting in vivo indicating anatomical vector barriers. Gene Ther. **6:**1520–1535.
25. **Gall, J., A. Kass-Eisler, L. Leinwand, and E. Falck-Pedersen.** 1996. Adenovirus type 5 and 7 capsid chimera: fiber replacement alters receptor tropism without affecting primary immune neutralizing epitopes. J. Virol. **70:**2116–2123.
26. **Hidaka, C., E. Milano, P. L. Leopold, J. M. Bergelson, N. R. Hackett, R. W. Finberg, T. J. Wickham, I. Kovesdi, P. Roelvink, and R. G. Crystal.** 1999. CAR-dependent and CAR-independent pathways of adenovirus vector-mediated gene transfer and expression in human fibroblasts. J. Clin. Investig. **103:**579–587.
27. **Hilkens, J., M. J. Ligtenberg, H. L. Vos, and S. V. Litvinov.** 1992. Cell membrane-associated mucins and their adhesion-modulating property. Trends Biochem. Sci. **17:**359–363.
28. **Hitt, M. M., C. L. Addison, and F. L. Graham.** 1997. Human adenovirus vectors for gene transfer into mammalian cells. Adv. Pharmacol. **40:**137–206.
29. **Horwitz, M. S.** 1996. Adenoviruses, p. 2149–2171. *In* B. N. Fields, D. M. Knipe, and P. M. Howley (ed.), Virology, vol. 2. Lippincott-Raven Publishers Inc., Philadelphia, Pa.
30. **Howard, D. S., D. A. Rizzierri, B. Grimes, D. Upchurch, G. L. Phillips, A. K. Stewart, J. R. Yannelli, and C. T. Jordan.** 1999. Genetic manipulation of primitive leukemic and normal hematopoietic cells using a novel method of adenovirus-mediated gene transfer. Leukemia **13:**1608–1616.
31. **Hsu, K.-H., K. Lonberg-Holm, B. Alstein, and R. L. Crowell.** 1988. A monoclonal antibody specific for the cellular receptor for the group B coxsackie-ieviruses. J. Virol. **62:**1647–1652.
32. **Huang, S., R. I. Endo, and G. R. Nemerow.** 1995. Upregulation of integrins $\alpha v \beta 3$ and $\alpha v \beta 5$ on human monocytes and T lymphocytes facilitates adenovirus-mediated gene delivery. J. Virol. **69:**2257–2263.
33. **Kaplan, J. M., S. E. Pennington, J. A. St. George, L. A. Woodworth, A. Fasbender, J. Marshall, S. H. Cheng, S. C. Wadsworth, R. J. Gregory, and A. E. Smith.** 1998. Potentiation of gene transfer to the mouse lung by complexes of adenovirus vector and polycations improves therapeutic potential. Hum. Gene Ther. **9:**1469–1479.
34. **Kirby, I., E. Davison, A. J. Beavil, C. P. Soh, T. J. Wickham, P. W. Roelvink, I. Kovesdi, B. J. Sutton, and G. Santis.** 1999. Mutations in the DG loop of adenovirus type 5 fiber knob protein abolish high-affinity binding to its cellular receptor CAR. J. Virol. **73:**9508–9514.
35. **Krasnykh, V. N., G. V. Mikheeva, J. T. Douglas, and D. T. Curiel.** 1996. Generation of recombinant adenovirus vectors with modified fibers for altering viral tropism. J. Virol. **70:**6839–6846.
36. **Lanuti, M., C. E. Kouri, S. Force, M. Chang, K. Amin, K. Xu, I. Blair, L. Kaiser, and S. Albelda.** 1999. Use of protamine to augment adenovirus-mediated cancer gene therapy. Gene Ther. **6:**1600–1610.
37. **Legrand, V., D. Spehner, Y. Schlesinger, N. Settelen, A. Pavirani, and M. Mehtali.** 1999. Fiberless recombinant adenoviruses: virus maturation and infectivity in the absence of fiber. J. Virol. **73:**907–919.
38. **Lieber, A., C.-Y. He, I. Kirillova, and M. A. Kay.** 1996. Recombinant adenoviruses with large deletions generated by Cre-mediated excision exhibit different biological properties compared with first-generation vectors in vitro and in vivo. J. Virol. **70:**8944–8960.
39. **Mathias, P., T. Wickham, M. Moore, and G. Nemerow.** 1994. Multiple adenovirus serotypes use αv-integrins for infection. J. Virol. **68:**6811–6814.
40. **McKay, T. R., L. J. MacVinish, B. Carpenter, M. Themis, S. Jezzard, R. Goldin, A. Pavirani, M. E. Hickman, A. W. Cuthbert, and C. Coutelle.** 2000. Selective in vivo transfection of murine biliary epithelia using polycation-

enhanced adenovirus. Gene Ther. **7:**644–652.

41. **Mei, Y. F., and G. Wadell.** 1995. Highly heterogeneous fiber genes in the two closely related adenovirus genome types Ad35p and Ad34a. Virology **206:** 686–689.

42. **Mei, Y. F., and G. Wadell.** 1995. Molecular determinants of adenovirus tropism. Curr. Top. Microbiol. Immunol. **199:**213–228.

43. **Michael, S. I., J. S. Hong, D. T. Curiel, and J. A. Engler.** 1995. Addition of a short peptide ligand to the adenovirus fiber protein. Gene Ther. **2:**660–668.

44. **Mittereder, N., K. L. March, and B. C. Trapnell.** 1996. Evaluation of the concentration and bioactivity of adenovirus vectors for gene therapy. J. Virol. **70:**7498–7509.

45. **Miyazawa, N., P. L. Leopold, and R. G. Crystal.** 2000. Adenovirus 7 fiber mediates lysis of a late endosomal compartment. Mol. Ther. **1:**S58.

46. **Miyazawa, N., P. L. Leopold, N. R. Hackett, B. Ferris, S. Worgall, E. Falck-Pedersen, and R. Crystal.** 1999. Fiber swap between adenovirus subgroups B and C alters intracellular trafficking of adenovirus gene transfer vectors. J. Virol. **73:**6056–6065.

47. **Mizuguchi, H., and M. A. Kay.** 1998. Efficient construction of recombinant adenovirus vectors by an improved in vitro ligation method. Hum. Gene Ther. **9:**2577–2583.

48. **Nemerow, G. R., and P. L. Stewart.** 1999. Role of α_v integrins in adenovirus cell entry and gene delivery. Microbiol. Mol. Biol. Rev. **63:**725–734.

49. **Persson, R., U. Svensson, and E. Everitt.** 1983. Virus receptor interaction in the adenovirus system. II. Capping and cooperative binding of virions on HeLa cells. J. Virol. **46:**956–963.

50. **Persson, R., C. Wohlfart, U. Svensson, and E. Everitt.** 1985. Virus-receptor interaction in the adenovirus system: characterization of the positive cooperative binding of virions on HeLa cells. J. Virol. **54:**92–97.

51. **Philipson, L., K. Lonberg-Holm, and U. Pettersson.** 1968. Virus-receptor interaction in an adenovirus system. J. Virol. **2:**1064–1075.

52. **Pring-Akerblom, P., A. Heim, and F. J. Trijssenaar.** 1998. Molecular characterization of hemagglutination domains on the fibers of subgenus D adenoviruses. J. Virol. **72:**2297–2304.

53. **Pring-Akerblom, P., and T. Adrian.** 1995. Characterization of adenovirus subgenus D fiber genes. Virology **206:**564–571.

54. **Rodriguez, E., and E. Everitt.** 1999. Adenovirus cellular receptor site recirculation of HeLa cells upon receptor-mediated endocytolysis is not low pH-dependent. Arch. Virol. **144:**787–795.

55. **Roelvink, P. W., A. Lizonova, J. G. Lee, Y. Li, J. M. Bergelson, R. W. Finberg, D. E. Brough, I. Kovesdi, and T. J. Wickham.** 1998. The coxsackievirus-adenovirus receptor protein can function as a cellular attachment protein for adenovirus serotypes from subgroups A, C, D, E, and F. J. Virol. **72:**7909–7915.

56. **Roelvink, P. W., I. Kovesdi, and T. J. Wickham.** 1996. Comparative analysis of adenovirus fiber-cell interaction: adenovirus type 2 (Ad2) and Ad9 utilize the same cellular fiber receptor but use different binding strategies for attachment. J. Virol. **70:**7614–7621.

57. **Roelvink, P. W., G. Mi Lee, D. A. Einfeld, I. Kovesdi, and T. J. Wickham.** 1999. Identification of a conserved receptor-binding site on the fiber proteins of CAR-recognizing adenoviridae. Science **286:**1568–1571.

58. **Romanczuk, H., C. E. Galer, J. Zabner, G. Barsomian, S. C. Wadsworth, and C. R. O'Riordan.** 1999. Modification of an adenoviral vector with biologically selected peptides: a novel strategy for gene delivery to cells of choice. Hum. Gene Ther. **10:**2615–2626.

59. **Scatchard, G.** 1949. The attraction of proteins for small molecules and ions. Ann. N. Y. Acad. Sci. **51:**660–672.

60. **Segerman, A., Y. F. Mei, and G. Wadell.** 2000. Adenovirus types 11p and 35p show high binding efficiencies for committed hematopoietic cell lines and are infective to these cell lines. J. Virol. **74:**1457–1467.

61. **Shayakhmetov, D. M., T. Papayannopoulou, G. Stamatoyannopoulos, and A. Lieber.** 2000. Efficient gene transfer into human CD34$^+$ cells by a retargeted adenovirus vector. J. Virol. **74:**2567–2583.

62. **Shenk, T.** 1996. Adenoviridae, p. 2111–2148. *In* B. N. Fields, D. M. Knipe, and P. M. Howley (ed.), Fields virology, vol. 2. Lippincott-Raven Publisher, Philadelphia, Pa.

63. **Singh, A. K., B. S. Kasinath, and E. J. Lewis.** 1992. Interaction of polycations with cell-surface negative charges of epithelial cells. Biochim. Biophys. Acta **1120:**337–342.

64. **Stevenson, S. C., M. Rollence, J. Marshall-Neff, and A. McClelland.** 1997. Selective targeting of human cells by a chimeric adenovirus vector containing a modified fiber protein. J. Virol. **71:**4782–4790.

65. **Stevenson, S. C., M. Rollence, B. White, L. Weaver, and A. McClelland.** 1995. Human adenovirus serotypes 3 and 5 bind to two different cellular receptors via the fiber head domain. J. Virol. **69:**2850–2857.

66. **Suzuki, Y.** 1994. Gangliosides as influenza virus receptors. Variation of influenza viruses and their recognition of the receptor sialo-sugar chains. Prog. Lipid Res. **33:**429–457.

67. **Thacker, T. C., and F. B. Johnson.** 1998. Binding of bovine parvovirus to erythrocyte membrane sialylglycoproteins. J. Gen. Virol. **79:**2163–2169.

68. **Tomko, R. P., R. Xu, and L. Philipson.** 1997. HCAR and MCAR: the human and mouse cellular receptors for subgroup C adenoviruses and group B coxsackieviruses. Proc. Natl. Acad. Sci. USA **94:**3352–3356.

69. **Von Seggern, D. J., C. Y. Chiu, S. K. Fleck, P. L. Stewart, and G. R. Nemerow.** 1999. A helper-independent adenovirus vector with E1, E3, and fiber deleted: structure and infectivity of fiberless particles. J. Virol. **73:**1601–1608.

70. **Wickham, T. J., D. M. Segal, P. W. Roelvink, M. E. Carrion, G. M. Lizonova, and I. Kovesdi.** 1996. Targeted adenovirus gene transfer to endothelial and smooth muscle cells by using bispecific antibodies. J. Virol. **70:**6831–6838.

71. **Wickham, T. J., P. Mathias, D. A. Cheresh, and G. R. Nemerow.** 1993. Integrins alpha v beta 3 and alpha v beta 5 promote adenovirus internalization but not virus attachment. Cell **73:**309–319.

72. **Xu, Z. Z., and G. W. Both.** 1998. Altered tropism of an ovine adenovirus carrying the fiber protein cell binding domain of human adenovirus type 5. Virology **248:**156–163.

73. **Zabner, J., A. Puga, P. Freimuth, and M. J. Welsh.** 1997. Lack of high affinity fiber receptor activity explains the resistance of ciliated airway epithelia to adenovirus infection. J. Clin. Investig. **100:**1144–1149.